Structural Consequences of Spin Conversion in a Sterically Encumbered Ni(II) Porphyrin

Kathleen M. Barkigia,[†] Nora Y. Nelson,[‡] Mark W. Renner,[†] Kevin M. Smith,[‡] and Jack Fajer*[,†]

Department of Applied Science, Brookhaven National Laboratory, Upton, New York 11973, and Department of Chemistry, University of California, Davis, California 95616

Received: July 21, 1999

The crystal structure of a pyridine-ligated, high-spin Ni(II) complex of 2,3,7,8,12,13,17,18-octabromo-5,15-bis(isopropyl)-10,20-bis(isopropylidenyl) porphyrin, **2**, is reported and compared to the unligated, low-spin Ni(II) complex, **1**, previously reported. The results demonstrate that conversion to high-spin Ni(II) in nonplanar, sterically encumbered porphyrins induces a significant core expansion about the Ni while nonplanarity is still retained. The expansion of the core parameters (Ni−N, Ct-Cα, Ct-C*meso*) and the Ni−N_{axial} distances are characteristic of the $d_{x^2-y^2}$ and d_{z^2} orbital occupancies in high-spin Ni(II) porphyrins and document the structural consequences of the spin conversion in severely nonplanar Ni(II) porphyrins. The stereochemical results are particularly relevant to ligation effects in nonplanar Ni biomolecules and synthetic porphyrins increasingly used as biomimetic models of conformational effects in chromophores and prosthetic groups in vivo, and to the remarkably wide range of lifetimes observed for excited (d,d) states in nonplanar, sterically constrained Ni(II) porphyrins in which the $d_{x^2-y^2}$ and d_{z^2} orbitals are also populated.

Introduction

Current interest in nickel porphyrins is prompted by the original identification of Factor 430 as the cofactor involved in the final steps of CO_2 conversion to hydrocarbon by methanogenic bacteria, and the more recent crystal structure of methyl-coenzyme M reductase that confirmed the identity of F430 and showed it to be a hexacoordinated Ni(II) tetrapyrrole.[1] Another nickel-containing porphyrinic biomolecule, tunichlorin, is found in algae-consuming marine invertebrates.[2] Although its biological configuration is unknown, it is very likely to also be axially ligated in vivo. Surprisingly, few structures of high-spin Ni(II) porphyrins have been reported[3−8] despite the additional interest in using Ni porphyrins as spectroscopic models and probes for heme conformations in proteins[9] and for biomimetic cytochrome P450 hydroxylations and epoxidations.[5] Indeed, the use of halogenated porphyrins as robust catalysts for P450 type reactions[5,10] led us to investigate the bromination of meso tetraalkylporphyrins with unexpected and novel consequences: reaction of Ni(II) 5,10,15,20-tetraisopropylporphyrin with Br_2 or NBS yielded the novel octabrominated compound **1**, a quinone dimethide resonance form of a porphyrin,[11] see Figure 1, whose identity was confirmed by X-ray crystallography.[12] The structural data also showed the compound to be a low-spin Ni(II) complex with significant distortions from planarity.[12] Halogenated and other electron-deficient Ni(II) porphyrins (including F430) readily bind axial ligands to form hexacoordinated high-spin Ni(II) complexes in which the d_{z^2} and $d_{x^2-y^2}$ orbitals are each singly populated.[1,4−8] We report here that **1** does indeed bind two axial pyridines and compare the stereochemical parameters of the ligated high-spin Ni(II) derivative, **2**, with those of the previously reported low-spin form.[12]

In a different context, the structural consequences of the spin conversion, especially the expansion of the core surroundings of the metal described here, are particular relevant to the photodynamics of Ni porphyrins. The nonplanar Ni(II) 5,10,-15,20-tetra (*tert*-butyl)- and tetraadamantylporphyrins (NiT(t-Bu)P and NiT(Ad)P), with conformations similar to those found here,[13] exhibit an unusually wide span of (d,d) excited-state lifetimes that range from picoseconds at room temperature to microseconds at 80 K.[13] As in the ligated species, the d_{z^2} and $d_{x^2-y^2}$ orbitals are also populated upon excitation of the low-spin Ni(II) ground state, and the relaxation of the expanded core of the (d,d) excited state is likely to strongly influence the decay back to the ground state in the sterically constrained nonplanar porphyrins, especially in frozen matrixes.[14]

Results and Discussion

The pyridine-ligated complex **2** proved difficult to crystallize and only thin crystals could be obtained. Nonetheless, a satisfactory refinement with good precision (esds are less than 0.01 Å) was obtained by taking advantage of synchrotron radiation (microcrystallography).[15]

The structural formula, structure, and atom names for the macrocycle of **2** are shown in Figure 1. The overall conformation of the molecule and the atom names for the pyridine axial ligands are illustrated in Figure 2. Displacements from planarity for **2** are displayed in linear form in Figure 3, and are further compared there in numerical form with those of **1**, the previously reported low-spin Ni(II) complex.[12] Bond distances are presented in Figure 4, and averaged bond distances and angles are listed in Table 1 where they are contrasted to those of **1**.

As is obvious from Figure 2, the two axial pyridines are the most salient feature of the new structure. The ligands are situated asymmetrically from the Ni at 2.207(5) Å and 2.153(5) Å for N6 and N5, respectively. The pyridines form an angle of 73° to each other and align along the clefts formed by the ruffled macrocycle (vide infra). The pyridine comprised of N6 is rotated

* Author to whom correspondence should be addressed at Department of Applied Science, Brookhaven National Laboratory, Upton, NY 11973-5000. Phone: (516) 344-4521. E-mail: fajerj@bnl.gov.

[†] Brookhaven National Laboratory.

[‡] University of California.

10.1021/jp992508y CCC: $18.00
Published on Web 09/25/1999

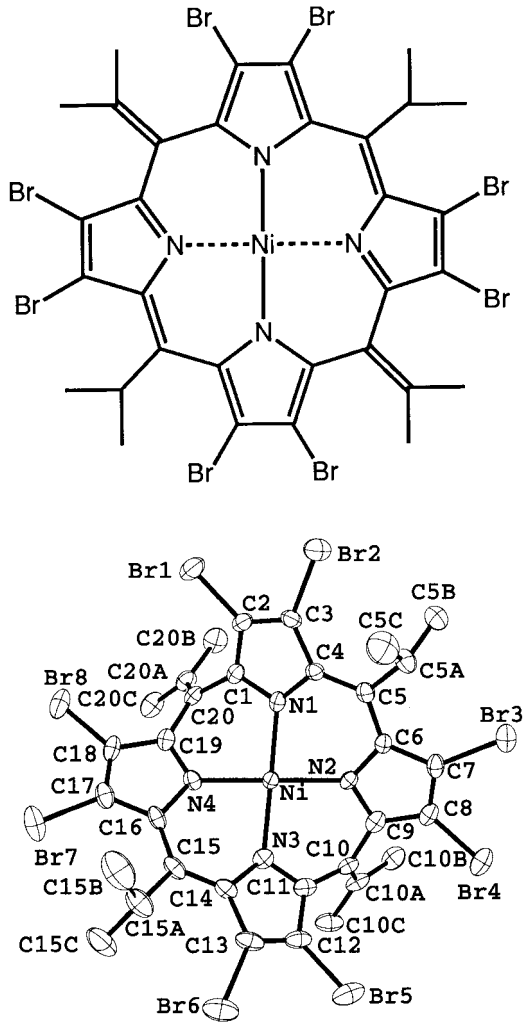

Figure 1. Structural formula, molecular structure, and atom names for the macrocycle of **2**. Thermal ellipsoids enclose 50% probability, and hydrogens are omitted for clarity.

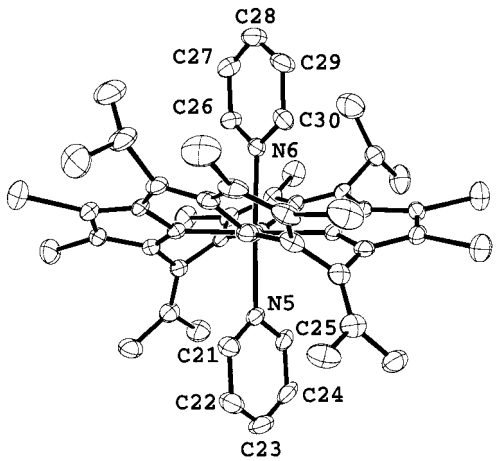

Figure 2. Edge-on view of **2** with its pyridine axial ligands. Ellipsoids enclose 50% probability.

40° from the N1−N3 axis and orients toward the C10−C20 axis of the meso carbons whereas the second pyridine is turned 33° to N1−N3 and orients toward the groove delineated by C5−C15.

The axial distances to the pyridines are typical of those found in other Ni(II) porphyrins with nitrogenous ligands which fall within the narrow range of 2.15−2.26 Å.[3,4,6−8] As well, in the sole synthetic Ni porphyrin with oxygenous ligands,[5] the Ni−O

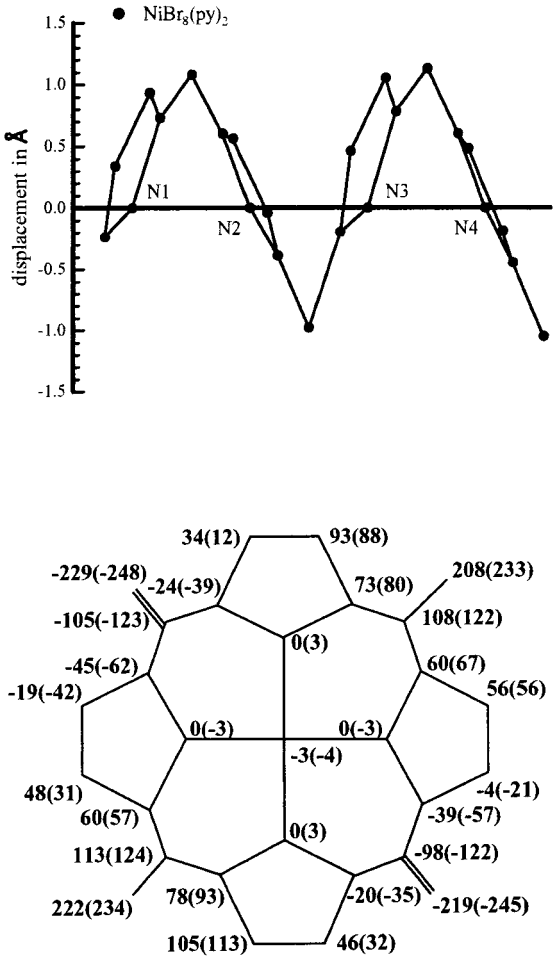

Figure 3. (Top) Linear display of the out-of-plane displacements of the core atoms of **2** from the plane defined by the 4 nitrogens. The horizontal axis is not to scale. (Bottom) Comparison of the out-of-plane displacements of the core atoms of **2** and **1** (in parentheses) from the planes of the 4 nitrogens, in units of 0.01 Å.

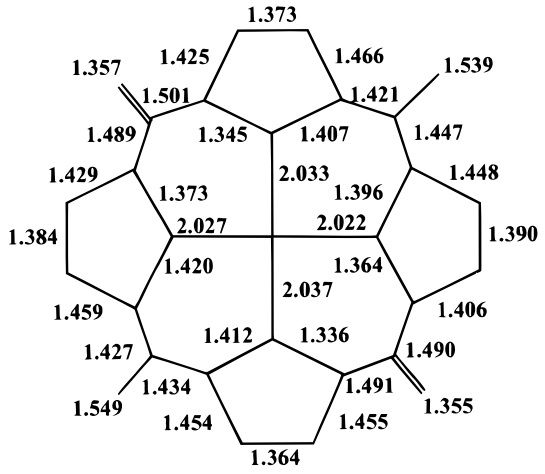

Figure 4. Bond distances for the macrocycle of **2**. Esds are 0.005 Å for the Ni−N distances and 0.009 Å for a typical C−C bond.

distances are 2.14 Å, and the axial distances for the oxygen and sulfur ligands of F430 in the protein[1] range between 2.1 and 2.4 Å. All of the above parameters are consonant with occupancy of the d_{z^2} orbital[3,4] as required by the high-spin Ni(II). The second unpaired electron in the latter resides in the $d_{x^2-y^2}$ orbital which, in turn, leads to expansion of the core around the Ni: the equatorial Ni−N distances to the pyrroles in **2** average 2.030(5) Å, a considerable increase relative to the

TABLE 1: Comparison of Distances (Å) and Angles (°) in 1 and 2

	2, high-spin[a]	**1**, low-spin[b]
Ni−N (porp)	2.030(5) Å	1.877(7) Å
Ni−N (ax)	2.153(5); 2.207(5)	
Cα−Cβ	1.443(9)	1.430(12)
Cβ−Cβ	1.378(10)	1.370(13)
Cβ−Br	1.896(6)	1.867(9)
Cα−Cm	1.432(9)	1.420(12)
Cα−Cm (DB[c])	1.493(9)	1.472(11)
N−Cα	1.409(7)	1.395(11)
N−Cα (DB)	1.350(8)	1.342(11)
Cm−CH$(CH_3)_2$	1.544(8)	1.525(12)
Cm−C$(CH_3)_2$ (DB)	1.356(9)	1.343(13)
Ct−N	2.030	1.869
Ct−Cα	3.08	2.91
Ct−Cα (DB)	2.96	2.86
Ct−Cm	3.22	3.17
Ct−Cm (DB)	3.43	3.29
N−Ni−N (opp)	178.1(2)°	175.6(3); 179.3(3)°
N−Ni−N (adj)	84.9(2)	87.4(3)
N−Ni−N (adj) (DB)	95.1(2)	92.6(3)
Cα−N−Cα	109.9(5)	109.4(7)
Ni−N−Cα	126.7(4)	122.5(5)−127.7(5)
Ni−N−Cα (DB)	120.3(4)	123.5(5)
Ni−N−Cα (av)	123.5(4)	124.5(5)
N−Cα−Cβ	105.7(5)	106.0(7)
N−Cα−Cβ (DB)	108.9(6)	109.5(7)
N−Cα−Cβ (av)	107.3(5)	107.7(7)
N−Cα−Cm	121.4(5)	121.2(7)
Cβ−Cα−Cm	131.4(5)	130.6(7)
Cα−Cm−Cα	123.8(5)	119.5(8)
Cα−Cm−Cα (DB)	114.9(5)	111.2(7)
Cα−Cβ−Cβ	107.8(5)	107.6(8)

[a] $T = 100$ K, this work. [b] $T = 130$ K, ref 12. [c] DB = at or closest to the exocyclic double bonds at C10 and C20.

average Ni−N distance of 1.877(7) Å in **1**, the low-spin state. Individually, the Ni−N distances vary from 2.022(5) to 2.037(5) Å and they fall well within the range of 2.00 to 2.07 Å reported for synthetic high-spin Ni porphyrins,[3−8] and the average of 2.09(4) Å found for F430.[1,16] The long equatorial Ni−N distances are thus clearly diagnostic of the $d_{x^2-y^2}$ orbital occupancy in the high-spin state of Ni(II). (NMR data further confirm that **2** is paramagnetic, see the Supporting Information.) Besides the increase in the Ni−N bonds, additional indicators of core expansion in **2** are the distances from the center of the 4 nitrogens (Ct) to the Cα and Cm positions. Compared to **1**, all of these are lengthened between 0.05 and 0.17 Å in **2**, see Table 1.

As illustrated in Figure 3, the macrocycle of **2** is highly distorted with large up-and-down, out-of-plane excursions of approximately a full angstrom at the meso positions and significant, asymmetric rotations of the pyrrole rings about the N2−N4 and N1−N3 axes. Such nonplanar distortions, particularly distinguished by the large meso carbon displacements, are defined as ruffled conformations, and are often found in sterically crowded low-spin Ni(II) porphyrins, including **1**.[6,9,12,13,17] A numerical comparison of the out-of-plane displacements in **1** and **2** is also presented in Figure 3. Clearly, both molecules exhibit similar deformations with **2** slightly less distorted, especially at the meso carbons.

Bond distances in **2** are displayed in Figure 4, and compared to those in **1** in Table 1. Equivalent bonds in **2** exhibit good correspondence across the 10,20-axis defined by the exocyclic double bonds and display unusual features compared to canonical porphyrins. The expected short double bonds of 1.356(9) Å of the 10,20-propylidenes are each flanked by long Cα−Cm bonds that average 1.493(9) Å. These, in turn, abut very short N−Cα bonds with average lengths of 1.350(8) Å. (Note that the latter are as short as the alkylidene double bonds.) In contrast, at the meso carbons C5 and C15, the distances of 1.544(8) Å to the isopropyl groups are typical of single bonds, the Cα−Cm bonds flanking them average 1.432(9) Å and their adjoining N−Cα bonds average 1.409(7) Å. Thus, in this contiguous pattern, the Cα−Cm and N−Cα bonds originating at the meso exocyclic single bonds at C5 and C15 are respectively shorter and longer than those evolving from the exocyclic meso double bonds at C10 and C20. Interestingly, this pattern appears to be characteristic of 5,15-dialkylideneporphyrins: comparable bonding schemes occur in **1** (see Table 1), and in the recently reported Zn 5,15- bis(dicyanomethylene)-10,20-bis(3,5-di-*tert*-butylphenyl)porphyrin.[18]

As noted in the Introduction, the sterically crowded Ni(II)T(t-Bu)P and Ni(II)T(Ad)P, with ruffled ground states conformations similar to **1**, exhibit an extraordinary range of excited (d,d) states with particularly long lifetimes of microseconds at 80 K compared to picoseconds at room temperature.[13] This remarkably wide span of excited-state lifetimes is not observed in planar Ni porphyrins whose (d,d) states typically last between 100 and 300 ps at all temperatures.[13] The present results clearly show that population of the $d_{x^2-y^2}$ and d_{z^2} orbitals (as would also occur in the excited (d,d) states) is accompanied by a significant structural expansion in the environment of the metal and in the porphyrin while the overall conformational landscape is generally maintained because the porphyrin macrocycle is sterically encumbered by the peripheral substituents. The long-lived excited states of the ruffled NiT(t-Bu)P and NiT(Ad)P at low temperatures thus imply that the relaxation of the (d,d) states is limited by severe steric constraints that hamper the structural readjustment to the short Ni−N distances[19] and concomitant macrocyclic "shrinking" of the low-spin Ni(II) ground states, i.e., a kinetic trapping mechanism with a large barrier for deactivation to the ground state.[13]

Drain et al.[13] have noted that the wide range of excited-state lifetimes of the ruffled Ni porphyrins suggests their potential use for molecular photonic applications. As well, other nonplanar porphyrins with β-octabromo substituents have recently been shown to exhibit reversible-saturable absorption[20] and the other recently synthesized dialkylidene porphyrin is also being considered for nonlinear optical applications.[18] The brominated Ni(II) dipropylidene porphyrins **1** and **2** can therefore also be expected to possess novel photodynamic properties, and these are presently being explored.

Acknowledgment. This work was supported by the Division of Chemical Sciences, U.S. Department of Energy, under Contract No. DE-AC02-98CH10886 at BNL and by National Science Foundation Grant No. CHE-96-23177 at UCD. We thank Dr. Jonathan C. Hanson for assistance with the crystallographic data collection.

Supporting Information Available: Experimental crystallographic details, atomic coordinates, bond distances and angles, anisotropic thermal parameters, and hydrogen coordinates for **2**; optical spectra in CH_2Cl_2 and pyridine, ^{1}H NMR spectra in $CDCl_3$ and pyridine-d_5 for **1** and **2**. This material is available free of charge via the Internet at http://pubs.acs.org.

References and Notes

(1) Ermler, U.; Grabarse, W.; Shima, S.; Goubeaud, M.; Thauer, R. K. *Science* **1997**, *278*, 1457, and references therein.

(2) Sing, H. L.; Bible, K. C.; Rinehart, K. L. *Proc. Natl. Acad. Sci. U.S.A.* **1996**, *93*, 10560. Pettit, G. R.; Kantoci, D.; Doubek, D. L.; Tucker, B. E. J. *Nat. Prod.* **1993**, *56*, 1981.

(3) Jia, S. L.; Jentzen, W.; Shang, M.; Song, X. Z.; Ma, J. G.; Scheidt, W. R.; Shelnutt, J. A. *Inorg. Chem.* **1998**, *37*, 4402.

(4) Duval, H.; Bulach, V.; Fischer, J.; Weiss, R. *Acta Crystallogr., Sect. C* **1997**, *53*, 10270. *Inorg. Chem.*, in press.

(5) Ozette, K.; Leduc, P.; Palacio, M.; Bartoli, J.-F.; Barkigia, K. M.; Fajer, J.; Battioni, P.; Mansuy, D. *J. Am. Chem. Soc.* **1997**, *119*, 6442.

(6) Renner, M. W.; Barkigia, K. M.; Melamed, D.; Smith, K. M.; Fajer, J. *Inorg. Chem.* **1996**, *35*, 5120.

(7) Balch, A. L.; Olmstead, M. M.; Phillips, S. L. *Inorg. Chem.* **1993**, *32*, 3931.

(8) Kirner, J. F.; Garofalo, J., Jr.; Scheidt, W. R. *Inorg. Nucl. Chem. Lett.* **1975**, *11*, 107.

(9) Shelnutt, J. A.; Song, X.-Z.; Ma, J.-G.; Jia, S.-L.; Jentzen, W.; Medforth, C. *J. Chem. Soc. Rev.* **1998**, *27*, 31, and references therein.

(10) Meunier, B. *Chem. Rev.* **1992**, *92*, 1411. Mansuy, D. *Coord. Chem. Rev.* **1993**, *125*, 129. Sheldon, R. A. *Metalloporphyrins in Catalytic Oxidations*; M. Dekker: New York, 1994. Groves, J. T.; Han, Y. Z. In *Cytochrome P450: Structure, Mechanism and Biochemistry*; Ortiz de Montellano, P., Ed.; Plenum Press: New York, 1995; p 3. Dolphin, D.; Traylor, T. G.; Xie, L. *Acc. Chem. Res.* **1997**, *30*, 251. Birnbaum, E. R.; Labinger, J. A.; Bercaw, J. E.; Gray, H. B. *Inorg. Chim. Acta* **1998**, *270*, 433. Ozette, K.; Battioni, P.; Leduc, P.; Bartoli, J. F.; Mansuy, D. *Inorg. Chim. Acta* **1998**, *272*, 4.

(11) **1** may be formally considered to be a porphodimethene. The closest porphodimethene analogue of **1**, Ni(II) 5,15-dimethyl-2, 3, 7, 8, 12, 13, 17, 18-octaethyl-5H,15H-porphyrin does not bind axial ligands and adopts a principally roof-like conformation: Dwyer, P. N.; Buchler, J. W.; Scheidt, W. R. *J. Am. Chem. Soc.* **1974**, *96*, 2789.

(12) Nelson, N. Y.; Medforth, C. J.; Khoury, R. G.; Nurco, D. J.; Smith, K. M. *Chem. Commun.* **1998**, 1687.

(13) Drain, C. M.; Gentemann, S.; Roberts, J. A.; Nelson, N. Y.; Medforth, C. J.; Jia, S.; Simpson, M. C.; Smith, K. M.; Fajer, J.; Shelnutt, J. A.; Holten, D. *J. Am. Chem. Soc.* **1998**, *120*, 3781.

(14) **1** and **2** were chosen to model the (d, d) excited-state orbital occupancies and resulting conformations of NiT(t-Bu)P and NiT(Ad)P because the latter do not bind axial ligands in the ground state, and because their sterically encumbered conformations resemble that of **1**.[13]

(15) $NiN_4C_{32}H_{26}Br_8 \cdot 2(C_5H_5N)$ crystallized from a mixture of pyridine/pentane in space group $P2_1/c$ with $a = 13.450(1)$ Å, $b = 19.845(1)$ Å, $c = 16.816(1)$ Å, $\beta = 96.05(1)°$, $V = 4463.4(5)$ Å^3, $Z = 4$. Because of the small crystal size, $0.14 \times 0.14 \times 0.013$ mm, data were collected at beamline X7B of the Brookhaven National Synchrotron Light Source with a MAR 345 image plate detector at $\lambda = 0.8798$ Å and $T = 100$ K. A total of 54607 reflections ($\pm h \pm k \pm l$) were measured in the range $3.94 \leq 2\theta \leq 62.38°$ with 7428 unique. Refinement with SHELXL93 yielded $R1 = 0.058$, w$R2 = 0.170$ for the 6869 data having $I > 2\sigma(I)$ and $R1 = 0.062$, w$R2 = 0.177$ for all data. Full experimental details are given in Table 1S of the Supporting Information which also includes complete sets of atomic coordinates, bond lengths and angles, anisotropic thermal parameters, and hydrogen coordinates in Tables 2S−5S, and a comparison of the out-of-plane displacements in **1** and **2** in linear form (Figure 1S). Also included therein are the optical spectra of **1** in CH_2Cl_2 and of **2** in neat pyridine (Figure 2S), and NMR spectra of **1** in $CDCl_3$ and 2 in pyridine-d_5 (Figure 3S). The green solution of **1** in CH_2Cl_2 with absorption bands at 482 nm and 596 nm[12] changes to bright pink in pyridine with absorption bands at 500 nm (sh.), 520 nm and a weak, broad absorption extending throughout the 600−800 nm region. The ^{1}H NMR spectrum of **1** in $CDCl_3$ features[12] two sets of methyl protons (δ 1.74 [d, 12H], 2.11 [s, 12H] and one set of isopropyl methine protons (δ 4.42 [septet, 2H]) which broaden and shift to 0.99 (br, 12H), 4.93 (s, 12H) and −1.33 (br, 2H).

(16) The longer Ni−N distances in high-spin F430 likely reflect its more planar conformation compared to that of **2**. In contrast, in an isolated low-spin F430, the Ni−N distances average 1.86(2) Å and the molecule is as distorted as **1**: Färber, G.; Keller, W.; Kratky, C.; Jaun, B.; Pfaltz, A.; Spinner, C.; Kobelt, A.; Eschenmoser, A. *Helv. Chim. Acta* **1991**, *74*, 697.

(17) Barkigia, K. M.; Nurco, D. J.; Renner, M. W.; Melamed, D.; Smith, K. M.; Fajer, J. *J. Phys. Chem. B* **1998**, *102*, 322.

(18) Blake, I. M.; Anderson, H. L.; Beljonne, D.; Bredas, J. L.; Clegg, W. *J. Am. Chem. Soc.* **1998**, *120*, 10764.

(19) In the low-spin Ni(II)T(t-Bu)P,[13] the Ni−N distances average 1.869-(7) Å, essentially the same as those in **1**, 1.877(7) Å.

(20) Su, W.; Cooper, T. M. *Chem. Mater.* **1998**, *10*, 1212.